Automated Monitoring System for Detection of Solar Radio Bursts for CALLISTO Spectrums

Nor Hazmin Sabri
Faculty of Science and Marine Environment, Universiti Malaysia Terengganu

Nur Zulaikha Mohd Afandi
East Coast Environmental Research Institute, Universiti Sultan Zainal Abidin

Roslan Umar
East Coast Environmental Research Institute, Universiti Sultan Zainal Abidin

Suhailan Safei
Faculty of Informatics and Computing, Universiti, Sultan Zainal Abidin

他

https://doi.org/10.5109/7323404

出版情報：Proceedings of International Exchange and Innovation Conference on Engineering & Sciences (IEICES). 10, pp.1158-1163, 2024-10-17. International Exchange and Innovation Conference on Engineering & Sciences
バージョン：

Automated Monitoring System for Detection of Solar Radio Bursts for CALLISTO Spectrums

Nor Hazmin Sabri[1*], Nur Zulaikha Mohd Afandi[2], Roslan Umar[2], Suhailan Safei[3], Christian Monstein[4]
[1]Faculty of Science and Marine Environment, Universiti Malaysia Terengganu, 21030 Kuala Nerus, Terengganu, Malaysia, [2]East Coast Environmental Research Institute, Universiti Sultan Zainal Abidin, 21300 Kuala Nerus, Terengganu, Malaysia, [3]Faculty of Informatics and Computing, Universiti, Sultan Zainal Abidin, 22200 Besut, Terengganu, Malaysia, [4]Istituto Ricerche Solari (IRSOL), Università della Svizzera Italiana (USI), CH-6605 Locarno-Monti, Switzerland.
Corresponding author email: norhazmin@umt.edu.my

Abstract: *Continuous monitoring of solar radio bursts using ground spectrometers is now essential for solar researchers, particularly in predicting space weather. Type II, Type III, and Type IV solar bursts are linked to significant solar flares and coronal mass ejections (CMEs), which affect Earth's magnetosphere and human activities. Since 2002, CALLISTO spectrometers have gathered data, available at e-Callisto.org, but detecting and classifying these bursts was labor-intensive. This study aims to enhance the monitoring of solar radio bursts (SRBT II, SRBT III, SRBT IV) by automating the CALLISTO system. The developed system includes three stages: burst-finder, burst-classifier, and monitoring. Tested on both pre-training and real data, it achieved 87% success in burst detection and 61% in burst classification. Results are displayed on the user-friendly website http://solar.myfik.net, providing a valuable tool for CALLISTO-based solar burst monitoring and supporting space weather forecasting research.*

Keywords: Automated Monitoring System; Coronal Mass Ejection (CMEs); Solar Radio Burst; Space Weather Forecasting; CALLISTO

1. INTRODUCTION

The Sun, amidst billions of stars in the Milky Way, serves as the radiant heart of our Solar System, illuminating its planets with hot plasma enveloped in a vast magnetic field predominantly composed of hydrogen and helium. Its influence extends profoundly to Earth and neighboring planets, shaping their climates and electromagnetic environments. Periodically, the Sun exhibits dynamic solar activity, marked by intense phenomena such as solar flares and coronal mass ejections (CMEs). These events unleash torrents of high-energy electrons and ionized atoms into space, capable of disrupting not only the solar environment but also perturbing Earth's magnetic field, occasionally triggering geomagnetic storms [1].

The emanations from these solar eruptions traverse interplanetary space alongside the solar wind, interacting with celestial bodies along their trajectory, engendering both transient and sustained disturbances. Solar flares, originating from sudden magnetic energy releases in active regions, and CMEs, stemming from colossal solar eruptions [2, 3, 4], are frequently accompanied by bursts of radio emissions known as solar radio bursts (SRBs). These bursts, categorized into five types based on their frequency characteristics, play a pivotal role in space weather research [7]. They encompass noise-storm bursts (Type I), slow-drift bursts associated with CMEs (Type II), fast-drift bursts from energetic particle movements (Type III), broad-band continuum emissions following Type II events (Type IV), and continuum emissions at meter wavelengths (Type V).

Type II bursts, characterized by a gradual frequency drift, are linked to shock waves propagating through the solar corona triggered by CMEs, while Type III bursts, featuring a rapid frequency drift, arise from accelerated charged particles escaping the Sun's magnetic field [5, 6, 8]. Type IV bursts, appearing post-Type II events, persist for extended durations and are attributed to electron spiraling within the solar corona's magnetic field.

The observation and classification of these SRB types are integral to forecasting space weather, as solar activity profoundly impacts technology and daily life on Earth [5, 6, 8]. The reliance on technology in modern society has spurred heightened efforts in monitoring solar activities using advanced radio receivers and magnetometers. However, the sheer volume and complexity of recorded solar radio spectra present significant challenges in effectively identifying and classifying SRBs, exacerbated by diverse burst shapes and spectral noise.

In response, researchers have increasingly focused on developing automated systems for detecting and categorizing solar radio bursts since the early 2000s. These systems aim to expedite and enhance the accuracy of SRB identification, offering timely insights for solar researchers and operational agencies. This study proposes the development of an automated monitoring system tailored specifically for detecting and classifying Type II, Type III, and Type IV SRBs with high precision. The system will integrate advanced signal processing algorithms and machine learning techniques to achieve robust detection capabilities. Importantly, it will provide real-time results accessible via a dedicated web interface synchronized with continually updated spectrum databases, facilitating rapid response to evolving solar conditions.

By advancing the automation of SRB detection and classification, this research seeks to bolster the efficacy of space weather forecasting and mitigate potential impacts on space missions, satellite operations, and terrestrial infrastructure.

2. METHODOLOGY

The methodology for developing the automated monitoring system for solar radio bursts begins with a comprehensive review and synthesis of foundational research on solar radio burst formation and underlying physics. This initial phase is crucial for establishing a robust understanding of the spectral characteristics and classification criteria essential for accurate detection and classification within the system.

The algorithmic framework for the automated system is implemented using MATLAB, selected for its computational robustness, versatility in handling various input spectrum formats, and efficient data manipulation capabilities through matrix operations. MATLAB's suitability for scientific computing ensures optimal performance in processing and analyzing large volumes of solar radio spectrum data.

The system operates through a structured workflow consisting of two primary processes. Initially, it accesses and extracts compressed '*.fit' image output spectra from the CALLISTO database, a comprehensive repository renowned for its extensive collection of solar radio emissions data. This database is configured to update automatically at 15-minute intervals, ensuring that the system incorporates the latest observational data available. Users have the flexibility to specify the date of interest for the input data retrieval, facilitating targeted analysis based on temporal variations in solar activity.

Upon extraction, the system seamlessly converts the compressed spectral data into an uncompressed format suitable for subsequent processing within the MATLAB environment. This preprocessing step prepares the data for rapid analysis and classification of solar radio burst types.

The algorithm then executes rapid spectral analysis, leveraging predefined detection and classification algorithms tailored to identify distinct types of solar radio bursts, including Type II, Type III, Type IV, and other relevant classifications. Upon detection, the system generates comprehensive output files formatted to include critical metadata such as station identifiers, timestamps of observations, maximum intensity measurements, geographic coordinates (latitude and longitude) of monitoring stations, and the categorized burst type.

To enhance usability and facilitate intuitive interpretation of results, the system integrates advanced visualization tools. A global representation visually maps the detected solar radio bursts across different CALLISTO stations, employing a color-coded scheme based on their respective maximum intensity values. This spatial visualization aids in identifying spatial patterns and hotspot regions of solar activity.

Furthermore, the system presents graphical displays depicting the maximum intensity measurements for each CALLISTO station, complemented by annotations indicating the specific type of detected bursts (Type II, Type III, Type IV, or others). These graphical representations provide a concise overview of solar activity dynamics at each monitoring location, enabling comparative analysis and trend identification.

Users can conveniently access and interact with the generated results through a dedicated web interface hosted at http://solar.myfik.net. The website is designed with a user-centric approach, featuring systematic layout and intuitive navigation to ensure accessibility and comprehension of complex solar radio burst data. This user-friendly interface enhances the dissemination and utilization of findings among researchers, operational agencies, and the broader scientific community.

2.1 Observational data

Following the development phase, the algorithm underwent rigorous training using a dedicated testing dataset. This dataset was meticulously curated to ensure comprehensive coverage of solar radio burst types (SRBT II, SRBT III, and SRBT IV) observed in CALLISTO spectra from 2014. The selection criteria prioritized spectra where the edges of solar radio bursts were distinctly clear, facilitating accurate training of the algorithm.

The training dataset consisted of 100 CALLISTO spectra manually classified based on observed bursts types. Specifically, 20 spectra were classified as Type II bursts (SRBT II), 34 as Type III bursts (SRBT III), and 14 as Type IV bursts (SRBT IV). In cases where multiple burst types occurred within a single spectrum, 7 spectra were categorized as having mixed burst types, while 10 spectra showed no discernible bursts, and 15 contained only noise.

To validate the algorithm's performance, each training dataset was cross-checked against authoritative sources, including the CALLISTO spectrum burst catalogue and daily solar activity reports from the Space Weather Prediction Center (SWPC), NOAA. Monthly burst activity reports compiled by Christian Monstein also served as a benchmark for comparison. This comprehensive validation process ensured the reliability and accuracy of the training data used to optimize the algorithm's detection capabilities.

Throughout the testing phase, the algorithm was evaluated against manually classified CALLISTO spectra from 2014. This testing dataset encompassed the entire spectrum of solar radio burst events recorded during that year, further verifying the algorithm's efficacy across diverse solar activity scenarios.

In cases where discrepancies or uncertainties arose regarding the algorithm's decision-making thresholds, iterative refinement cycles were conducted. The MATLAB code underlying the algorithm's design concept was systematically reviewed and revised to enhance detection accuracy. Successive iterations continued until the algorithm consistently achieved a satisfactory detection rate exceeding 80%, demonstrating robust performance in identifying and classifying SRBT II, SRBT III, and SRBT IV bursts.

All outcomes, including training results, algorithm adjustments, and performance metrics, were meticulously documented and analysed. The iterative development process ensured that the algorithm effectively leveraged machine learning principles and signal processing techniques to accurately discern solar radio burst signatures from complex spectral data.

2.2 Pre-processing

The initial stage of the data processing algorithm focuses on optimizing data visualization by mitigating unwanted signals inherent in solar radio burst spectra. Upon reading the input data spectrum, several critical steps are undertaken to prepare the data for accurate analysis and interpretation.

Firstly, the algorithm initiates a comprehensive check for missing values within the data spectrum. If no missing values are detected, indicating data completeness, the spectrum proceeds to the next processing stages. In cases where missing values are identified, the corresponding data spectrum is removed from further analysis to maintain data integrity and reliability.

Subsequently, the algorithm standardizes the size of the data spectrum to ensure uniformity across all input datasets. This involves adjusting the spectrum's dimensions by either adding or removing columns and rows as necessary. Any added columns or rows are populated with a default value of 0 to maintain consistency in data structure and facilitate subsequent computational operations.

Following size standardization, the algorithm implements background cancellation techniques to further refine the data spectrum. This critical step involves subtracting the local mean intensity observed during daylight periods from the global background mean intensity recorded during nighttime or periods of minimal solar activity. By nullifying background noise and environmental interference, this process enhances the clarity and accuracy of signal detection within the spectrum.

Together, these sequential steps in the data processing algorithm—checking for missing values, standardizing spectrum size, and applying background cancellation—form the foundational framework for optimizing data visualization in solar radio burst analysis. This meticulous preprocessing approach aims to streamline subsequent data interpretation and facilitate insightful visualization of solar activity dynamics.

2.3 Burst detection

The automated system for solar radio burst classification employs three primary characteristics (C1, C2, C3) based on intensity values measured across temporal and frequency domains within the spectrum. These characteristics serve as foundational criteria for assessing the presence and attributes of solar bursts, ensuring robust detection and classification.

C1 evaluates the temporal occurrence of solar bursts within the spectrum, primarily determined through manual observation and analysis. It quantifies the differences between the average intensity values across each temporal channel (column) and the overall average intensity value spanning the entire time range (Dt(diff)). The criterion for C1 to be considered true is met when these differences exceed a predefined threshold value, reflecting significant temporal variations indicative of solar burst activity.

C2 focuses on the frequency occurrence of solar bursts within the spectrum, also assessed through manual observation and calculation. It involves comparing the average intensity values across each frequency channel (row) with the average intensity value across the entire frequency range (Df(diff)). Similar to C1, C2 is validated when these differences surpass a specified threshold value, highlighting pronounced frequency fluctuations associated with solar burst emissions.

C3 encompasses two sub-conditions that evaluate the intensity variations between both temporal and frequency channels within the spectrum. This criterion aims to refine burst resolution by enhancing the system's sensitivity to intensity changes indicative of solar activity. By scrutinizing intensity differences across channels, C3 enhances the accuracy and reliability of burst detection capabilities.

In the decision-making process, the automated system identifies a positive solar burst event when either all three primary characteristics (C1, C2, and at least one sub-condition of C3) or at least two out of the three characteristics are validated as true. This comprehensive approach ensures a robust assessment of solar burst phenomena, accounting for temporal, frequency, and intensity dynamics observed within the spectrum.

Upon confirming the presence of a solar burst based on these criteria, the system proceeds to the next stage of burst classification. This classification phase leverages predefined algorithms and machine learning models to categorize detected bursts into specific types (e.g., Type II, Type III, Type IV), thereby facilitating comprehensive analysis and interpretation of solar radio burst data.

2.4 Burst classification

The burst-classifier algorithm is designed to categorize detected solar radio bursts into three specific types: SRBT II, SRBT III, and SRBT IV. Developed through a synthesis of solar burst theory principles and curve fitting techniques, the algorithm exclusively processes positive burst results obtained from intensity measurements across both temporal and frequency channels.

Classification 1 adapts the theory of frequency drift calculation by integrating information from both frequency and temporal channels. This approach enhances the algorithm's ability to discern characteristic frequency drift patterns exhibited by Type II solar radio bursts, providing a quantitative basis for classification.

In Classification 2, the algorithm employs Gaussian nonlinear least squares curve fitting techniques. This methodology is applied to the mean intensity observed across the frequency channel. By fitting Gaussian curves to intensity data, cl2 aims to identify and classify Type III solar radio bursts, which are characterized by rapid frequency drifts typically associated with energetic particle accelerations in solar flares.

Similarly, Classification 3 utilizes Gaussian nonlinear least squares curve fitting, but this time applied to the mean intensity observed in the temporal channel. This approach enhances the algorithm's capability to detect Type III solar radio bursts based on temporal intensity variations indicative of dynamic plasma processes in the solar corona.

Classification 4 calculates the Sum of Squares Due to Error (SSE) value from polynomial curve fitting of intensity variations across the frequency channel. This statistical approach helps quantify the accuracy of polynomial models fitted to the observed intensity data, facilitating the classification of Type IV solar radio bursts characterized by broad-band continuum emissions.

In contrast, Classification 5 computes the SSE value from polynomial curve fitting of intensity variations across the temporal channel. This methodological step assists in identifying Type IV solar radio bursts based on temporal intensity characteristics, providing additional insights into the burst's temporal evolution and duration.

Together, these five classifications (cl1 to cl5) form the foundational framework of the burst-classifier algorithm. By integrating theoretical insights from solar burst physics with advanced curve fitting techniques, the algorithm enables precise categorization and analysis of

detected solar radio burst events. Each classification parameter leverages specific methodologies tailored to capture distinct burst characteristics across temporal and frequency domains, thereby supporting comprehensive research in solar physics and space weather forecasting.

3. RESULT AND DISCUSSION

In this study, we have documented a Solar Radio Burst (SRB) of Type III observed in the radio spectrum of Banting, Malaysia, on April 11, 2022. As per the solar and geophysical report provided by SWPC, NOAA, this Burst Type III event occurred from 05:11 to 05:16 UT, lasting for a duration of 5 minutes. During this event, the frequency exhibited a drift rate of 0.67 MHz per second (Figure 1).

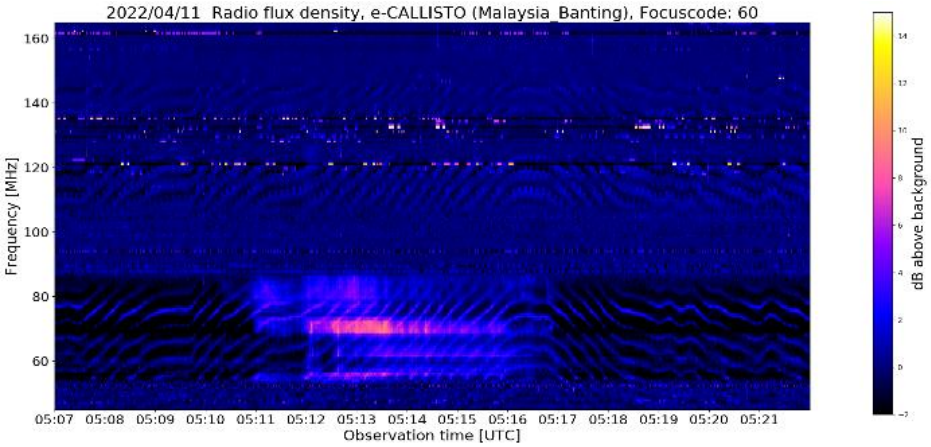

Fig. 1. Type III observed in the radio spectrum of Banting, Malaysia, on April 11, 2022.

Upon reading the .fit file in MATLAB, it became apparent that the file contained multiple instances of noise, manifesting as horizontal lines on the spectrum. To rectify this issue, the file underwent a standardization process where the noise was eliminated through background cancellation. Subsequently, the size of the spectrum, which initially consisted of 200 rows and 3600 columns, was reduced to a more manageable 200 rows and 900 columns. All these processes can be observed in Figure 2.

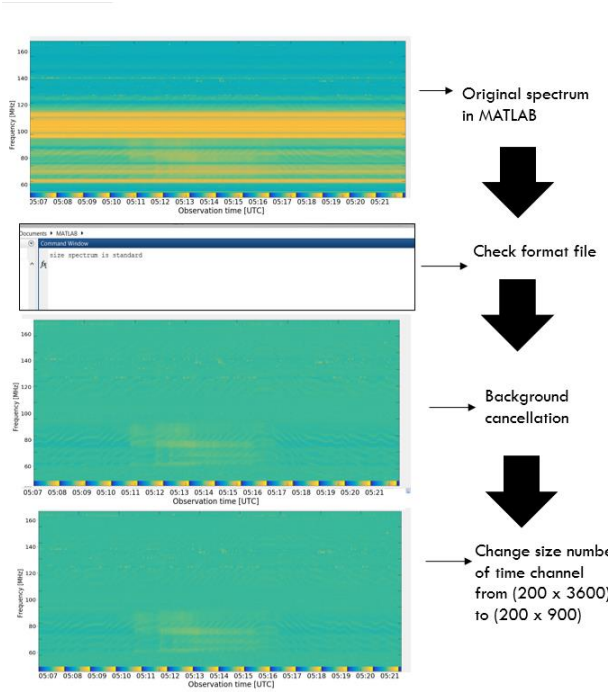

Fig. 2. The pre-processing process for CALLISTO Banting, Malaysia, on April 11, 2022.

For Burst Type III, the differences in average intensity values for each time channel (column) compared to the average intensity value for the entire time range (Dt(diff)) exhibit an increasing consistent pattern, with increasing flux observed from 05:10 to 05:15 UT (Figure 3(a). On the other hand, the differences in average intensity values for each frequency channel (row) compared to the average intensity value for the entire frequency range (Df(diff)) display two distinct peaks in flux, occurring in the frequency range of 80 to 100 MHz (Figure 3(b)).

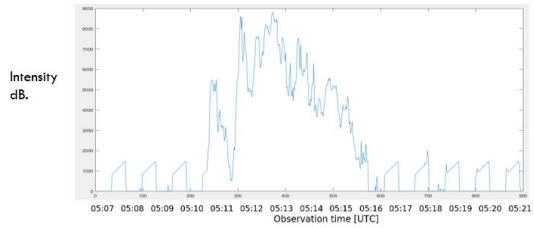

(a)

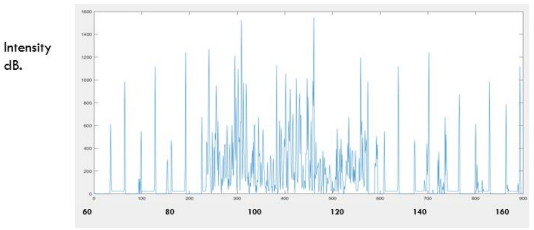

(b)

Fig. 3. Differences between average value intensity for each time channel (column) and average value intensity for all ranges of time, Dt (diff) in (a), while (b) differences between average value intensity for each frequency channel (row) and average value intensity for all ranges of frequency, Df (diff).

Subsequently, the flux of the spectrum was enhanced to improve visualization and aid in classification. This enhancement is clearly depicted in Figure 4, where Burst Type III is prominently visible on the spectrum visible on the spectrum.

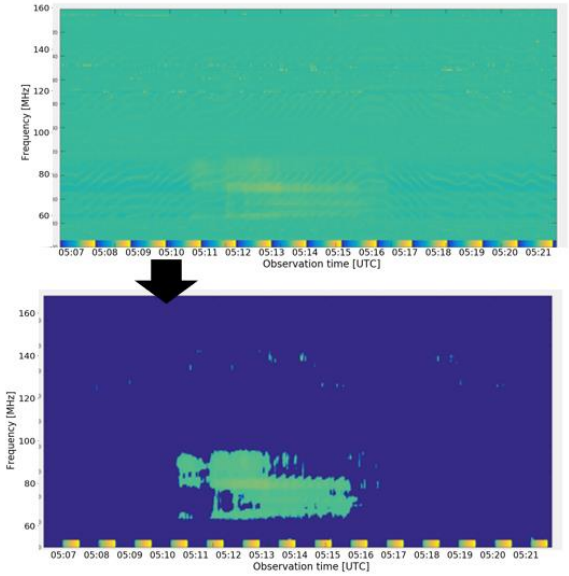

Fig. 4. The intensity of the spectrum was enhanced to get better resolution for bursts on the spectrum CALLISTO Banting, Malaysia, on April 11, 2022.

The curve fitting technique employed here is the Gaussian function, which is calculated using the equation specified. The predictions made using this Gaussian function are constrained within a 95% confidence interval. The coefficient 'c' in this equation represents the Gaussian RMS width, determining the width of the 'bell curve' utilized for comparison. Gaussian curve fitting is applied to both channels, and it is configured to fit a single peak using the bisquare robust method, which minimizes the weighted sum of squares as Figure 5. The value of 'c' is crucial in identifying the width of the curve, aligning with theoretical burst characteristics. The process involves identifying the value of 'c' specifically for the frequency channel. Once 'c' is determined, the decision-making step follows. In this step, the value of 'c1' is compared with a predefined threshold for three types of bursts, likely to be SRBT II, SRBT III, and SRBT IV.

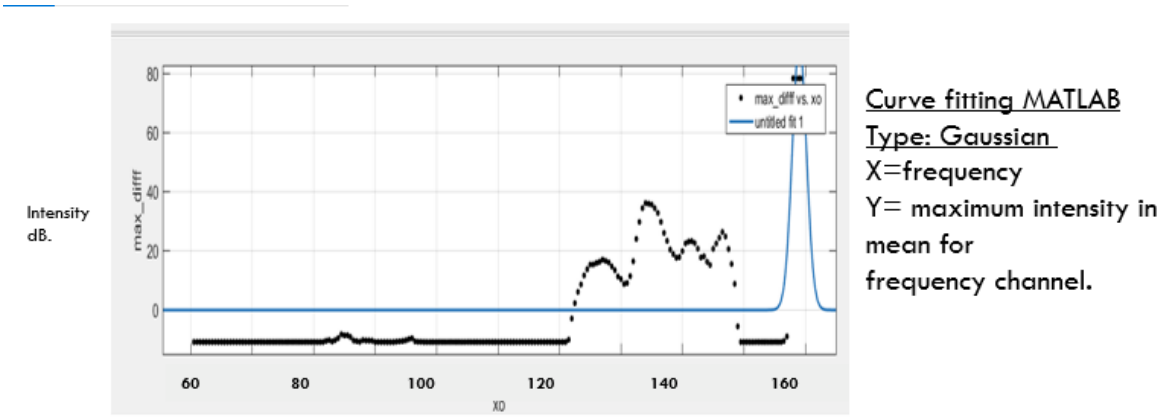

Fig. 5. The Gaussian curve fitting applied in the spectrum.

For Burst Type III, all parameters identified as characteristic of this type of burst were collected and consolidated. Following this, the fourth step in the process entails automatically reading and displaying positive bursts.

4. CONCLUSION

This study presents a web-based automated monitoring system for solar radio bursts of Type II, III, and IV using CALLISTO spectra. The primary aim is to assist solar radio researchers in analysing and documenting these bursts, providing a user-friendly, time-saving, and efficient alternative to manual observations. This system has the potential to revolutionize solar burst monitoring and may serve as a reference for both researchers and solar enthusiasts. Additionally, the development of the solar radio burst detection and classification algorithm, explained here and based on physical observations, holds promise for broader applications. It successfully detected 87% of solar radio bursts and classified them with a 61% success rate in testing data, with processing times of about 2 minutes and a maximum of 30 hours for full processing. The system handles a vast amount of CALLISTO spectra, making data retrieval and processing seamless and accessible through the solar.myfik.net website.

5. REFERENCES

[1] D. E. Morosan, E. K. Kilpua, E. P. Carley, C. Monstein, Variable emission mechanism of a Type IV radio burst, Astronomy & Astrophysics. 623 (2019) A63.

[2] E.P. Carley, N. Vilmer, P.J. Simões, B.Ó. Fearraigh, Estimation of a coronal mass ejection magnetic field strength using radio observations of gyrosynchrotron

radiation, Astronomy & Astrophysics. 608 (2017) A137.
[3] V. Vasanth, Y. Chen, S. Feng, S. Ma, G. Du, H. Song, X. Kong, B. Wang, an eruptive hot-channel structure observed at metric wavelength as a moving Type-IV solar radio burst, Astrophys. J. Lett. 830, (2016) L2.
[4] V. Vasanth, Y. Chen, M. Lv, H. Ning, C. Li, Feng, S. Z. Wu, G. Du, Source imaging of a moving Type IV solar radio burst and its role in tracking coronal mass ejection from the inner to the outer corona, Astrophys. J. 870 (2019) 30.
[5] N. Ramli, Z. S. Hamidi, Z. Z. Abidin, S. N. Shahar, The Relation between solar radio burst Type II, III and IV due to solar activities, 2015 International Conference on Space Science and Communication (IconSpace), (2015) 123-127.
[6] N. Gopalswamy, Interplanetary radio bursts. In Solar and Space Weather Radiophysics: Current Status and Future Developments, Springer Netherlands (2004) 305-333.
[7] M. R. Kundu, Solar Radio Astronomy, Wiley, New York,1965.
[8] E. W. Cliver, S. W. Kahler, D. V. Reames, Coronal shocks and solar energetic proton events. The Astrophysical Journal, 605(2) (2004) 902.